Neurosurgical Craniotomy Localization Using Interactive 3D Lesion Mapping for Image-Guided Neurosurgery

ZHIYU DAI[1], RONGQIAN YANG [2,3,4], FEI HANG[1], JIAN ZHUANG[5], QINYONG LIN[1], ZHIGANG WANG[6], AND YONGHUA LAO[2]

[1]School of Medicine, South China University of Technology, Guangzhou 510006, China
[2]Department of Biomedical Engineering, South China University of Technology, Guangzhou 510006, China
[3]School of Medicine, Yale University, New Haven, CT 06520, USA
[4]Guangdong Engineering Technology Research Center for Translational Medicine of Mental Disorders, Guangzhou 510370, China
[5]Department of Cardiac Surgery, Guangdong Cardiovascular Institute, Guangdong General Hospital, Guangdong Academy of Medical Science, Guangzhou 510080, China
[6]Guangzhou Aimooe Technology Co., Ltd., Guangzhou 510006, China

Corresponding authors: Rongqian Yang (bmeyrq@foxmail.com) and Fei Hang (hfei@scut.edu.cn)

ABSTRACT Precise craniotomy localization is essential in neurosurgical procedures, especially during the preoperative planning. The mainstream craniotomy localization method utilizing image-guided neurosurgery system (IGNS) or augmented reality (AR) navigation system require experienced neurosurgeons to point out the lesion margin by probe and draw the craniotomy manually on the patient's head according to cranial anatomy. However, improper manual operation and dither from the AR model will bring in errors about craniotomy localization. In addition, there is no specific standard to evaluate the accuracy of craniotomy. This paper attempts to propose a standardized interactive 3D method using orthogonal transformation to map the lesion onto the scalp model and generate a conformal virtual incision in real time. Considering clinical requirements, the incision can be amended by 3D interaction and margin modification. According to the IGNS and the virtual incision, an actual craniotomy will be located on the patient's head and the movement path of the probe will be recorded and evaluated by an indicator, which is presented as an evaluated standard to measure the error between virtual and actual craniotomies. After the experiment, an incision is drawn on a 3D printing phantom based on the generated virtual one. The results show that the proposed method can generate a lesion-consistent craniotomy according to the size of the lesion and the mapping angle and delineate the incision on the patient's head precisely under the IGNS.

INDEX TERMS Craniotomy localization, image-guided neurosurgery, interactive 3D lesion mapping, octree decomposition, margin modification.

I. INTRODUCTION

Accurate craniotomy localization is recognized as a key for the success of minimally invasive neurosurgery [1]. The knowledge of anatomical location about lesions and the development of the incision localization contribute essentially to reduce mortality and morbidity of neuro-surgery [2]. Precise craniotomy not only reduces patient trauma, but also facilitates postoperative recovery. Meanwhile, localization has brought two issues: (1) where the incision must be planned in the scalp and (2) how to determine the size and shape of incision. Ideally, the neurosurgeon will design an incision that will allow access to all the relevant parts of the anatomy but minimize the extent of brain that is exposed [3]. In fact, only according to Computed Tomography (CT) or Magnetic Resonance (MR) images, it is not convenient for surgeons to precisely determine the shape and position of the incision. The utilization of image-guided neurosurgery system (IGNS) combined with a

Z. Dai *et al.*: Neurosurgical Craniotomy Localization Using Interactive 3D Lesion Mapping for Image-Guided Neurosurgery

IEEE*Access*

three-dimension (3D) incision localization is expected to achieve the above goals.

Multiple methods have focused on defining the correct size and position of the skin incision. Frame-based, stereotactic localization was the common technology with the lower rate of neurological deficits and complications in the past. [4]. Due to the inconvenience and the low accuracy, it has gradually given way to frameless IGNS in the late 1980s. IGNS quickly became an essential neurosurgical tool for craniotomy. Thus, some publications exploited frameless IGNS to locate lesion, design surgical route or control lesion resection in neurosurgical routine and mentioned that one of the most valuable applications of frameless IGNS was the localization of the craniotomy [6]. Wagner *et al.* [7] pointed out that in 40% of cases that had been performed by intraoperative IGNS, the system was only needed to define the size and position of the craniotomy. Mahvash *et al.* [8] showed that the mean error of the craniotomy localization significantly larger using conventional planning, but image guided surgery can reduce error and prevent oversized craniotomy. Therefore, the frameless IGNS should be popularized for craniotomy localization.

During the cranial procedure, the IGNS is used to accurately visualize the shape and spatial location of lesion in the virtual reconstructed brain, providing a wealth of anatomical information to surgeons for preoperative planning. A prerequisite for the reliable use of IGNS is the registration between the preoperative image obtained from CT or MR images and the intraoperative patient's anatomy. This step is called patient-to-image registration, whose purpose is to find the transformation relationship between the two coordinate systems [9]. When an eligible registration is achieved, the position of a surgical probe with extensive line will be tracked accurately and rendered in the IGNS view. Then, surgeons will use dots to outline the tumor relying on extensive line of probe's tip and connects these to create the contour of the tumor on the patient's head for a custom-tailored skin incision [10].

At present, a common method for craniotomy localization is based on commercial navigation system with augmented reality (AR). AR allows merging surgical field from the real environment with virtual information and vice versa [11]. Combined with a head-up display (HUD), neurosurgeons could observe virtual lesion through ''3D model views'' or ''silhouette views'' in real surgical view of the microscope and use the probe to draw the skin incision on patient's head [12], [13]. Unfortunately, the lesion model would dither in the HUD view caused by optical marker mistaken recognition, resulting in the manual errors occur and the incision to be oversize or undersize. Additionally, the lesion silhouette view is superimposed directly into the surgical field but lacks spatial information. Thus, it is difficult to accurately quantify the size and position of the designed incision without specific standard. Moreover, a literature review on AR-based surgical neuronavigators was presented; there are no prospective studies showing a significant difference

between AR-aided surgeries versus navigation-guided procedures in terms of morbidity, mortality, and clinical effectiveness [14]. Therefore, this paper attempts to propose an IGNS-based standardize method to address two main issues, namely, (1) determining the size and shape of craniotomy on the scalp relying on the lesion margin with optimization algorithm in real time; (2) delineating the actual incision by the IGNS and providing a probe's tip record method to evaluate the two craniotomy boundaries.

Compared with the mainstream method, our proposed method designs the incision preoperatively and delineates it on the patient's head through IGNS to reduce the effect of manual errors or image dither. It is divided into three parts, including preprocessing, mapping, and delineation. In the preprocessing phase, the scalp and lesion are segmented out from the patient's preoperative CT images (CTs) and reconstructed into a 3D model that stored as a point cloud. At the mapping step, we use orthogonal transformation to map the boundary of the lesion onto the screen to generate a mask image of lesion margin with same size as the rendering window in virtual space. Then, according to the coordinate transformation between world system and screen system as well as the mask image, the corresponding point cloud on the scalp is extracted and modified to generate a virtual incision for meeting clinical requirements. Meanwhile, the position of the incision is determined based on anatomy information by 3D interaction. At last, under the IGNS, the craniotomy would be delineated on the patient's head using the tracked probe, whose tip would be recorded to construct a new opening in the virtual space. The new craniotomy will compare with the previous one to evaluate its accuracy.
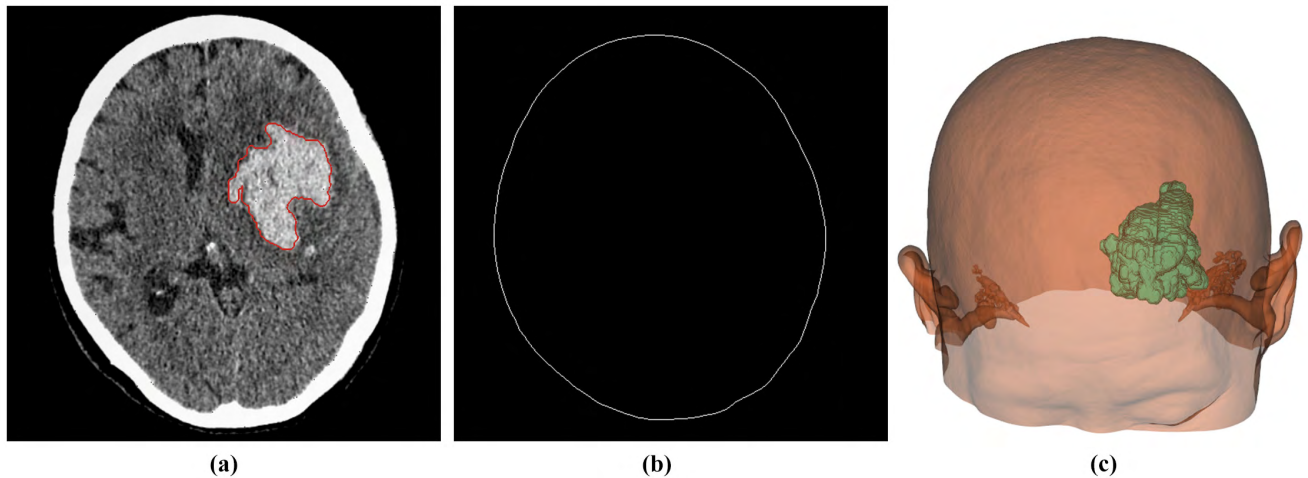
The rest of the paper is organized as follows: Section II introduces the workflow of the proposed craniotomy localization method, including medical image acquisition and processing, the mapping from lesion onto scalp accelerated by octrees, and the assessment about the craniotomy delineation. Section III describes experimental results about the running time and accuracy of our method. Section IV and V discuss the significance of the proposed method and conclude avenues of future work.

II. CRANIOTOMY LOCALIZATION
A. MEDICAL IMAGE ACQUISITION AND PROCESSING
To obtain the virtual 3D models, a small brain lesion dataset was built. This dataset included 8 cases with 3101 CTs. All image data were acquired through TOSHIBA Aquilion PRIME performed at the first affiliated hospital of Sun Yat-sen University. The mode we use is helical scan and the thickness of each slice is 0.5mm to meet the needs of the IGNS. Next, we segmented and visualized the 3D scalps and lesions.

Segmentation is significant for identifying region of interest (ROI) in medical images. Before medical 3D reconstruction, the relevant ROI anatomical image was efficiently obtained from the raw CTs by threshold and Fast Marching

IEEE *Access*

Z. Dai *et al.*: Neurosurgical Craniotomy Localization Using Interactive 3D Lesion Mapping for Image-Guided Neurosurgery

FIGURE 1. Image segmentation and visualization: (a)Segmenting the lesion by fast-marching; (b) Extracting the scalp by threshold; (c) 3D reconstruction of the lesion and scalp with MC algorithm.

method [15]. Due to some outliers in the raw image, they were removed with an anisotropic diffusion filter, which can preserve edges while smoothing image [16]. The CT value of the scalp differs from that of other anatomical structures, therefore we used threshold method to extract the scalp. While the lesion is similar to the soft tissue, its boundary is blurred and cannot be obtained by the threshold, thus we considered to use fast marching with pyramid algorithm [17]. At first, original images are downsampled based on pyramid algorithm, and then the fast-marching method is used to segment the lesion on the low-resolution images, which can improve remarkably the speed of segmentation. After obtaining the lesion margin on the low-resolution images, it is regarded as seed points of images which are upsampled to the high-resolution images. The margin was corrected continuously with the fast marching until the resolution is the same as the original images. The segmented results are shown in Fig. 1(a-b).

Medical image reconstruction is mainly based on 3D data and the workstation must support 3D interaction functions which allow the real-time exploration of 3D data [18]. According to segmented results, we obtained the image data of scalp and lesion. These two-dimensional (2D) images are then processed to obtain a single slice of 3D by merging two 2D image slices using the Marching Cubes algorithm [19]. Thereafter, the 3D model of scalp and lesion can be reconstructed and visualized. Fig. 1(c) shows the result of the reconstruction. By the way, the 3D visualization of scalp must cover at least the whole brain with the help of the rotation function, so that the 3D model of lesion can map flexibly to the scalp.

B. MAPPING FROM THE LESION TO THE SCALP
1) COORDINATE TRANSFORMATION
If the information of brain lesion requires to be transferred onto the scalp model, the transformation of coordinate system between polygonal data and viewing window should

be determined first. For convenience, there are five coordinate systems including modeling-coordinate system S_m, the world-coordinate system S_w, the camera-coordinate system S_c, the normalized coordinate system S_n and the screen-coordinate system S_s, which indicate that how 3D models projected onto the screen by coordinate conversion. Each model is created with its own S_m to specify the location of vertexes and then placed in the S_w to describe relative position between the models. To explain the rigid transformation between S_m and S_w, let p_c and p_w be the coordinates of an arbitrary vertex in S_m and S_w, respectively and the corresponding equation as follows:
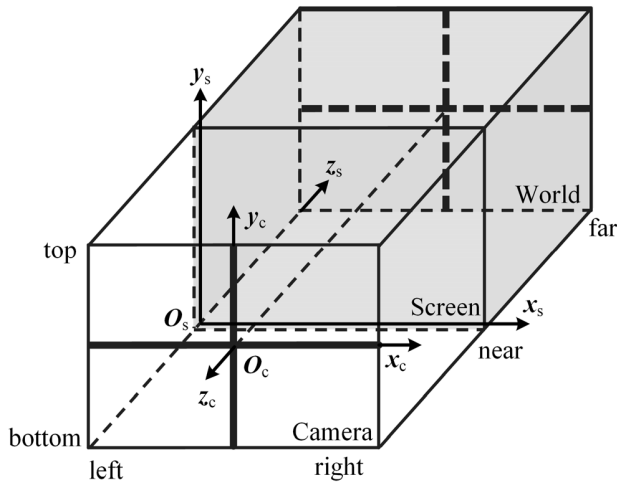
$$p_w = R_{mw}p_m + T_{mw} \qquad (1)$$

where R_{mw} represents a 3×3 rotation matrix and T_{mw} is a 3×1 translation vector.

Models in the S_w should be captured by a virtual camera model and projected to the screen. To ensure the accuracy of the projection, the camera model is described as an ideal orthographic camera, as shown in Fig. 2, with custom extrinsic parameters including a rotation matrix R_{wc}, a translation vector T_{wc} and a cuboid viewing frustum. The origin O_c in S_c is set at the center of viewpoint, and z_c is parallel to the optical axis. x_c and y_c align with the direction of x_s and y_s in S_s, respectively. Since the result of model rendering depends on the position and orientation of camera, the transformation relationship between S_c and S_w can be obtained from

$$p_c = R_{wc}p_w + T_{wc} \qquad (2)$$

According to the extent of viewing frustum, each 3D coordinate point in the S_c is converted to the S_n by using an orthogonal transfer matrix M_{norm}. Thus, the transformation equation as follows:

$$\begin{bmatrix} x_n & y_n & z_n & 1 \end{bmatrix}^T = M_{norm} \begin{bmatrix} x_c & y_c & z_c & 1 \end{bmatrix}^T \qquad (3)$$

Z. Dai *et al.*: Neurosurgical Craniotomy Localization Using Interactive 3D Lesion Mapping for Image-Guided Neurosurgery

IEEE *Access*

FIGURE 2. The structure of orthographic camera, including a cuboid viewing frustum (the gray part). Only objects inside the frustum can be displayed on the screen.

where M_{norm} is a 4×4 transfer matrix as follow:

$$M_{norm} = \begin{bmatrix} \dfrac{2}{x_{max}-x_{min}} & 0 & 0 & -\dfrac{x_{max}+x_{min}}{x_{max}-x_{min}} \\ 0 & \dfrac{2}{y_{max}-y_{min}} & 0 & -\dfrac{y_{max}+y_{min}}{y_{max}-y_{min}} \\ 0 & 0 & \dfrac{2}{z_{near}-z_{far}} & \dfrac{z_{near}+z_{far}}{z_{near}-z_{far}} \\ 0 & 0 & 0 & 1 \end{bmatrix}$$

Meanwhile, any position p_n (x_n,y_n,z_n) in S_n would be projected onto the screen orthogonally. Due to the lack of z-axis in 2D screen, the z coordinate values within symmetric viewing frustum are renormalized on the range from 0 to 1.0 for use in the visibility determination procedures. This allows the screen to be referenced as $z = 0$, and the transformation from the S_n to S_s is

$$\begin{bmatrix} x_s & y_s & z_s & 1 \end{bmatrix}^T = M_{screen} \begin{bmatrix} x_n & y_n & z_n & 1 \end{bmatrix}^T \quad (4)$$

where M_{screen} is a 4×4 transfer matrix as follow:

$$M_{screen} = \begin{bmatrix} \dfrac{x_{max}-x_{min}}{2} & 0 & 0 & \dfrac{x_{max}+x_{min}}{2} \\ 0 & \dfrac{y_{max}-y_{min}}{2} & 0 & \dfrac{y_{max}+y_{min}}{2} \\ 0 & 0 & \dfrac{1}{2} & \dfrac{1}{2} \\ 0 & 0 & 0 & 1 \end{bmatrix}$$

According to Eqs. (1-4), each vertex of model can be mapped onto the screen so that the screen coordinates and the outline of models can be obtained, and vice versa [20].

2) LESION MARGIN EXTRACTION AND PROCESSING

The purpose of extracting the lesion margin is to determine the location and extent of incision within the scalp.

Directly utilizing Eqs. (1-4), the screen coordinates of lesion can be obtained. However, the lesion model is wire-frame, causing the screen coordinates to be discrete, and it is difficult to extract the margin of lesion. As a result of above facts, an approach for extracting lesion margin is presented.

The first step is the pretreatment of coordinates. Only the margin points should be preserved, so the points inside the lesion would be removed to simplify extraction algorithm. The entire coordinates of lesion are divided into a grid whose size is the bounding box of the lesion. Then, the simplification of point set is realized with an 8-neighborhoods traversal operator. When coordinates all exist in 8 neighboring cells of the operator, indicating that points in the center cell are not on the margin, that points would be removed (Fig. 3(a)). Subsequently, the remaining points are constructed to a series of triangular grids using the Delaunay algorithm [21]. According to these triangular grids, the connection between the vertices would be obtained, and then a fast margin-detection algorithm is adapted to lesion margin extraction.
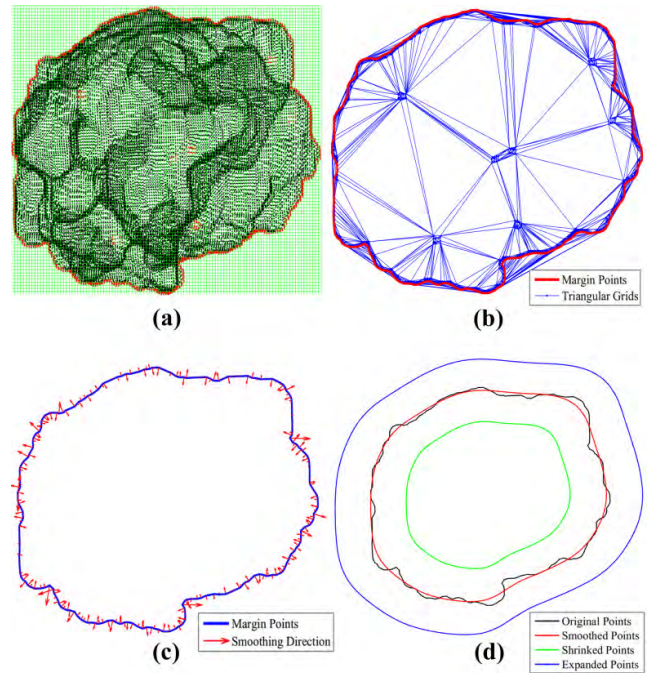
FIGURE 3. Lesion margin processing: (a) grid construction and margin points rough extraction; (b) the result of Delaunay and margin points accurate extraction; (c) smoothing direction calculation; (d) results of smoothed, shrinked and expanded points.

In the process of margin extraction, it is important to compare the angle relationship between the vectors composed of vertices in the triangular grids for detecting lesion margin. We have the following algorithm.

As shown in the Fig. 3(b), the lesion margin in the screen-coordinate system can be readily derived based on the Margin-Detection algorithm.

In practical clinic application, the size of craniotomy needs to be amended based on the position and size of lesion. Occasionally, if the lesion is small, the incision should be

IEEE *Access*

Z. Dai *et al.*: Neurosurgical Craniotomy Localization Using Interactive 3D Lesion Mapping for Image-Guided Neurosurgery

expanded to avoid the instruments get stuck and facilitate lesion resection. As for the large one, a larger opening is generated in general. However, it leads to more exposure of the brain that would increase the complications rate. Therefore, neurosurgeons apply the keyhole concept to design a smaller opening for the large lesion. Looking through a keyhole, one can overlook the interior of the brain with a sector visual field [22]. In additions, too complicated lesion margin is not conducive to surgeons designing the opening. Considering the clinic situation, we designed the following algorithm to smooth and modify the lesion margin for the convenience of surgeons.

In this algorithm, the number of iterations *iter* will affect the smoothness of margin and the final vector *v* can be calculated by above algorithm to control the smoothing direction (see Fig. 3(c)). Besides, the step length *s* will influence the rate of smoothing. Thus, these parameters need to be set by surgeons according to clinic requirements. Based on the above smoothing algorithm, the lesion margin will be easier for surgeons to operate. Combined the above concept of keyhole, the size of margin can be modified by the ratio *a*. When the ratio *a* is greater than 1, the lesion margin will expand, otherwise it shrinks (see Fig. 3(d)). We can set this parameter to control the size of margin for the incision modification. Next, the processed margin will be used as a mask for lesion mapping.

3) OPTIMIZATION ALGORITHM FOR CRANIOTOMY GENERATION

Calculating the mapping from lesion to screen, directly using the Eqs. (1-4), is feasible and accurate. Thanks to the large number of points in the scalp model, it is time consuming to compute screen coordinates of model. To extract the relevant points on the virtual skin rapidly. An optimization algorithm called octree decomposition is introduced to divide the scalp model and accelerate the craniotomy generation.

An octree is a hierarchical data structure that represents point cloud stored by the 3D polygonal model information in an eight-way branching tree [23]. The root node of the tree depicts a cubic space called minimum bounding box which includes the whole 3D object. The first level of the octree is composed of eight nodes also known as octants. Their child nodes are formed by halving bounding box along each axis direction, and so are child nodes in the next level. Nodes are classified into three types that are full, empty and partial, depending on the status about occupied by the object [24]. Each partial node is recursively subdivided into eight octants until all its leaf nodes are filled by the object completely or isolated from the object, or the default threshold value is not less than the maximum number of points per octant.
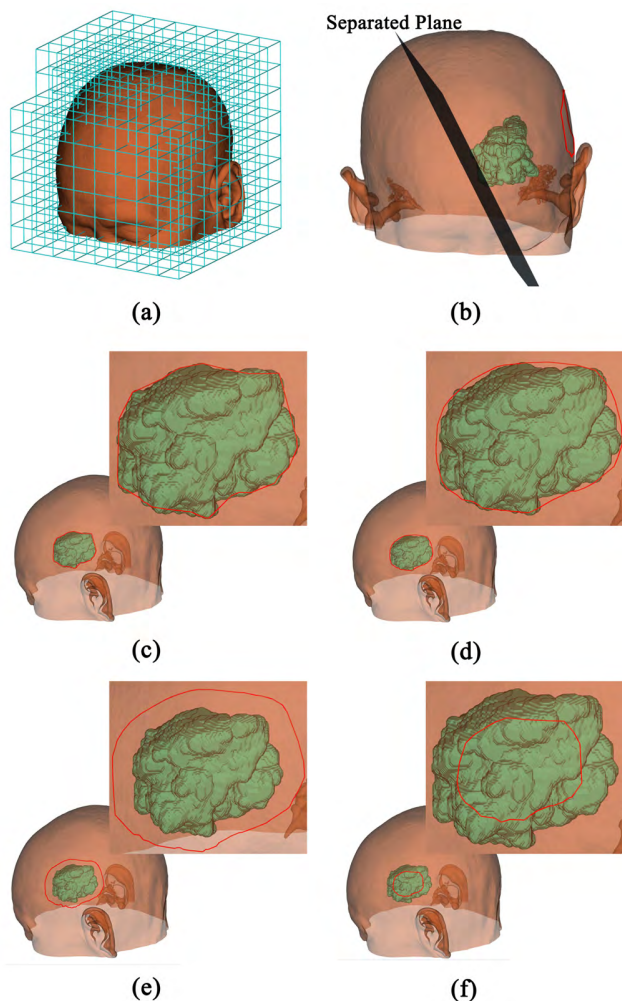
During the mapping calculating phase, the point cloud of scalp is divided iteratively according to the octree algorithm. Every octant contains eight vertices that indicate the size of space occupied by the point cloud. Next, eight vertices of the octant expressed by $V = \{v_i | i = 1, \ldots, 8\}$ are mapped onto the screen to acquire the corresponding coordinates
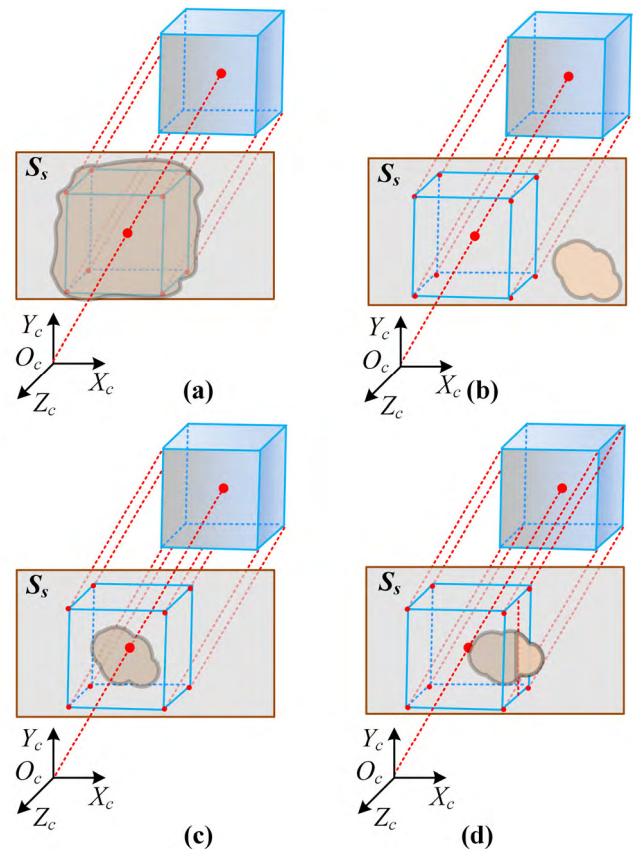
FIGURE 4. Forms of nodes: (a) full node; (b) empty node; (c) and (d) are partial node with mask outline completely and partly inside the boundary of octant's mapping on the screen, respectively.

$U = \{u_i | i = 1, \ldots 8\}$ in S_s by Eqs. (1-4), According to the mask image, pixels are divided into the inside and outside of the lesion. If a point p_w from point cloud is transformed by Eqs. (1-4) and its screen coordinates p_s is located within the mask image, the point p_w will be preserved. Similarly, if the screen point set U from eight vertices V falls completely inside the lesion, the entire point cloud in the octant will be saved in Fig. 4(a), otherwise it will be eliminated in Fig. 4(b). With respect to these octants filled partially by point cloud (partial node) would be subdivided to distinguish the different kinds of child in Fig. 4(c-d). Whether octants are retained, deleted, or continue to subdivide, can be determined by the relationship between the vertices screen coordinates U and mask image.

After the point cloud of scalp is divided in Fig. 5(a), we need to distinguish the front and back of the scalp with the lesion as the boundary, because there is no depth information in a 2D mask. By setting a plane as the separated plane that parallel to the view plane and goes through a lesion point farthest from the screen, all octants in front of the separated plane and within the lesion are retained (see Fig. 5(b)). Eventually, the mapped points from the lesion would be constructed into a surface and the margin of surface would be extracted regarded as the craniotomy on the scalp (Fig. 5(c)).

Z. Dai *et al.*: Neurosurgical Craniotomy Localization Using Interactive 3D Lesion Mapping for Image-Guided Neurosurgery

IEEE *Access*

FIGURE 5. Craniotomy generation: (a) the 3D scalp model decomposed with a 3-level octree; (b) a separated plane is set up for lesion mapping; (c) the craniotomy generated by lesion mapping directly; (d-f) craniotomies generated from the smoothed, expanded and shrinked points, respectively.

The craniotomy, at the same time, can be amended by a real-time 3D interaction. Besides, applying the Algorithm 1 and 2, we can obtain a smoothed, expanded or shrinked craniotomy to meet surgical requirements (Fig. 5(d-f)).

C. CRANIOTOMY DELINEATION

At the delineation step, an IGNS should be established to draw the generated craniotomy onto patient's head by the probe, as well as to evaluate difference between the two of craniotomy outline in virtual space. Current commercial navigation systems lack moving path record and calculation about the probe, thus we set up an IGNS with a record module. According to the module, the position of the probe's tip can be recorded to form a trace when the probe moves along the virtual boundary.

After a good patient-to-image registration is achieved, the probe is tracked and displayed on the screen. The module is

---

Algorithm 1 Margin-Detection Algorithm: Lesion Margin Search for Extraction

Input: lesion remaining point set P_{in}; connected triangular grids G; distance threshold t.
Initialize: Set initial point p_s be the point with the minimum x in P_{in}; Add a point above p_s into the end of P_{in} as the previous point p_{prev}; Set p_s as the current point p_{cur}.

1.   **while** $p_{cur} \neq p_s$ **do**
2.   Compute unit vector v_c from p_{prev} to p_{cur};
3.   Compute all unit vectors v_i from p_{cur} to the vertices of G and remove the v whose length is greater than t;
4.   Save these vectors v_i into an array V;
5.   **foreach** $v_i \in V$ **do**
6.   Calculate the angle α between v_c and v_i along the clockwise direction;
7.   Find a point with the minimum angle value as the next margin point p_{next};
8.   **end**
9.   Delete the connection between p_{cur} and the vertices from G to avoid repeated lookups;
10. Save p_{cur} into the point set P_{out};
11. Set p_{cur} to be p_{prev} and set p_{next} to be p_{cur};
12. **end**
Output: lesion margin point set P_{out}.

Algorithm 2 Margin-Modification Algorithm: Lesion Margin Smoothing

Input: lesion margin point set P_{in}; number of iterations *iter*.
Initialize: Set initial number of neighboring points n; Set step length of margin point movement s; Set the increment j of number of neighboring points; Compute the mean radius r_{in} of P_{in}.

1.   **for** $i = 1$ **to** *iter* **do**
2. $n = n + j$
3.   Extend n points to the beginning and end of P_{in};
4.   **for** $i = n+1$ **to** *length of* $P_{in} - n$ **do**
5.   Calculate two mean value coordinates p_1 and p_2 from two neighboring point set p_{i-r} to p_{i-1} and p_{i+1} to p_{i+r}, respectively;
6.   Compute unit vector v_1 from p_i to p_1 and unit vector v_2 from p_i to p_2;
7.   Obtain the final vector $v = v_1 + v_2$ and save it into vector set V
8.   **end**
9. $P_{out} = P_{in} + s*V$;
10. Compute the mean radius r_{out} of P_{out};
11. Compute the ratio a by $a = r_{in} / r_{out}$ and modify P_{out} by a to avoid the size is reduced.
12. **end**
Output: lesion margin point set P_{out}.

---

started when surgeons point the probe to the patient's head. Subsequently they can draw craniotomy outlines on the scalp

IEEE Access

Z. Dai *et al.*: Neurosurgical Craniotomy Localization Using Interactive 3D Lesion Mapping for Image-Guided Neurosurgery

while looking at the virtual tip to adjust the probe. When the tip returns to the origin, a virtual closed curve will be formed, and an actual craniotomy will be generated on the scalp. The two curves are consistent; hence, the virtual craniotomy is regarded as a duplicate from the actual one in virtual space and named the drawn craniotomy to distinguish the generated craniotomy. To evaluate the delineation error, a method is proposed for mean distance measurement between the two virtual craniotomies. More specifically, it first samples two outlines to take the point sets of them and let $C_D = \{p_i | i = 1, \ldots, n\}$ and $C_G = \{q_j | j = 1, \ldots, m\}$ be the point sets of the drawn craniotomy and generated craniotomy. Secondly, it traverses each point p_i in C_D to find the closest point q_k from C_G. Then, the point q_k connects q_{k-1} and q_{k+1} to draw line segments $l_{k-1,k}$ and $l_{k,k+1}$. Thirdly, it selects the minimum distance d_i from p_i to line segments $l_{k-1,k}$, and $l_{k,k+1}$, which would be built a set of distances $D_{DG} = \{d_i | i = 1, \ldots, n\}$. Similarly, the minimum distance g_j between the q_j in C_G and curve from C_D would be collected to build a set $D_{GD} = \{g_j | j = 1, \ldots, m\}$. Finally, the mean distance d_{mean} would be calculated as the standard for delineation error evaluation. The error equation as follow:

$$d_{\mathrm{mean}} = \frac{\frac{1}{n}\sum_{i=1}^{n} d_i + \frac{1}{m}\sum_{j=1}^{m} g_j}{2} \quad (5)$$

III. RESULT

To implement our proposed method, we established an IGNS that consists of an optical tracking system with a tracked probe and a navigation system which includes a workstation and two monitors. The overview of the IGNS is shown in Fig. 6. The IGNS is manufactured by Aimooe, Inc. (Guangzhou, China). More detail information can be seen at: https://www.aimooe.com. The accuracy of tracking is depended on patient-image space registration accuracy. With respect to probe tip localization, the accuracy of the probe is typically configuration dependent, and the above parameters have been reported in our previous research [25]. A navigation software is integrated in workstation that is Lenovo ThinkStation P410 with an Intel Xeon E5-2620 at a 2.10 GHz CPU and a 16GB RAM, supporting GPU accelerated 3D graphic rendering. Two monitors show navigation interface with anatomy information as well as the position of the tracked probe. Moreover, a 3D printing head phantom with six reflective markers, based on one of 8 actual CTs, is used for simulation of craniotomy delineation in real surgery.

A. EVALUATION OF CRANIOTOMY GENERATING TIME

Since our proposed method was implemented with 3D models of lesion and scalp, we segmented and reconstructed 8 CTs to display the relative position between lesion and skin in virtual space. According to the position of the lesion, surgeons were asked to select different perspectives that based on patient's anatomy for each CTs to locate the best craniotomy. Then we compared the running time between the proposed method
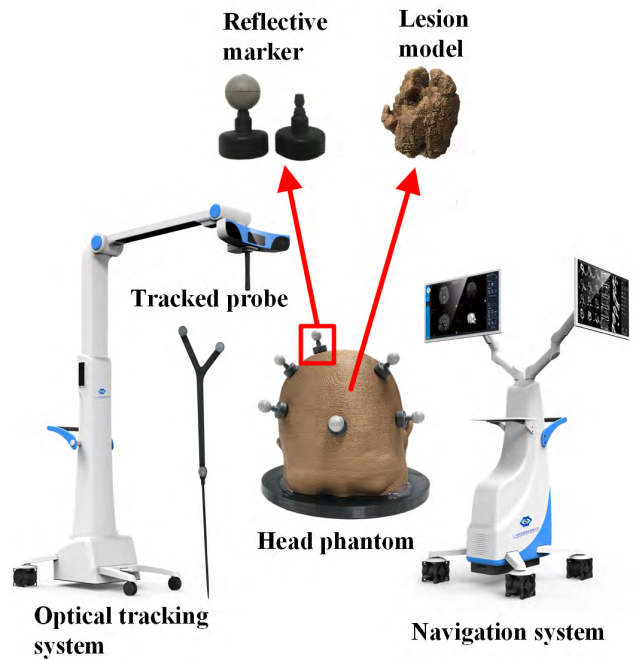

FIGURE 6. Overview of image-guided neurosurgery system and the appearance of the 3D printing head phantom.

and a method calculating all points of the scalp directly by Eqs. (1-4).

Fig. 7 illustrates the results of 3D surface reconstruction and craniotomy boundary about the 8 raw CTs. A surface is formed by extracting the points of scalp which intersect with the mask image generated by the lesion mapping in screen coordinate system. Then the contour of the surface was extracted to construct the cranial opening on the skin. Besides, all lesions were surrounded by boundaries from the selected perspectives.

TABLE 1. Time comparison between proposed craniotomy localization method and the method without octree.

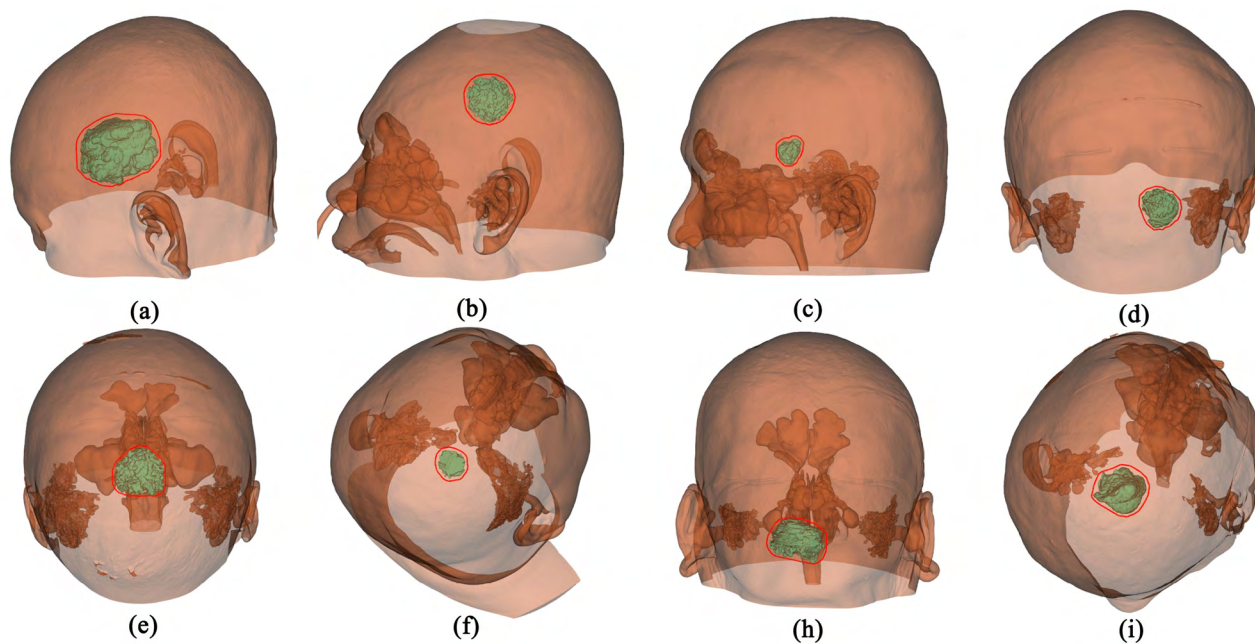| No.	Pathology	Lesion Points	Scalp Points	Without octree method Time (ms)	Proposed method Time (ms)
1	Hematoma	43750	732876	8251	504
2	Hematoma	18746	1087590	11186	464
3	Meningioma	7156	1135851	12993	671
4	Metastasis	20376	823681	9482	280
5	Pineocytoma	32856	959145	11103	408
6	Meningioma	9718	1472394	16987	750
7	Neuroma	30870	1023953	11850	424
8	Hematoma	34576	1153311	13518	515
Mean		24756	1046828	11921	502

Lesion **points** = points' number of the 3D lesion model.
Scalp **points** = points' number of the 3D scalp model
Craniotomy **points** = point's number of the 3D craniotomy result

Table 1 shows a summary of running time by two methods with octree and without octree. From the table1, the mean

Z. Dai *et al.*: Neurosurgical Craniotomy Localization Using Interactive 3D Lesion Mapping for Image-Guided Neurosurgery

IEEE *Access*

FIGURE 7. 3D surface reconstruction and craniotomy design. (a)-(i) are the results from 8 cases.

running time is reduced from 11921 to 502 ms, which is equal to about 96% of the mean time saved. The method without octree needs to traverse all points of scalp, so its runtime depends mainly on the number of scalp's points. The more points, it is more time consuming. Although the runtime of proposed method is also affected by the points' number of scalp and lesion, it is generally negligible compared to the method without octree. Therefore, our craniotomy localization method can basically be achieved in real time.

B. ACCURACY OF CRANIOTOMY DELINEATION

In the simulation of craniotomy delineation, we used the tracked probe to delineate an outline on the phantom along the virtual opening boundary under the guidance of the IGNS. Simultaneously, the record module was activated to evaluate the accuracy of craniotomy delineation. Thereafter, the error between two craniotomies was calculated according to Eq. (5).

In the phantom, the lesion model represents a left temporo-parietal hematoma. By the position of the lesion, a left temporal craniotomy was generated by our proposed method in virtual space (see Fig. 8(a)). After patient-to-image registration with good accuracy, as shown in Fig. 8(b), a closed craniotomy curve was drawn on the phantom. Fig. 8(c) exhibits two craniotomies, of which the red is the designed one, and the blue is the movement path of the probe. The two craniotomies are perfectly consistent based on the error analysis on YOZ plane (Fig. 8(d)). In addition, the value of d_{mean} is 0.71mm, which explains it is a proper operation for this case.
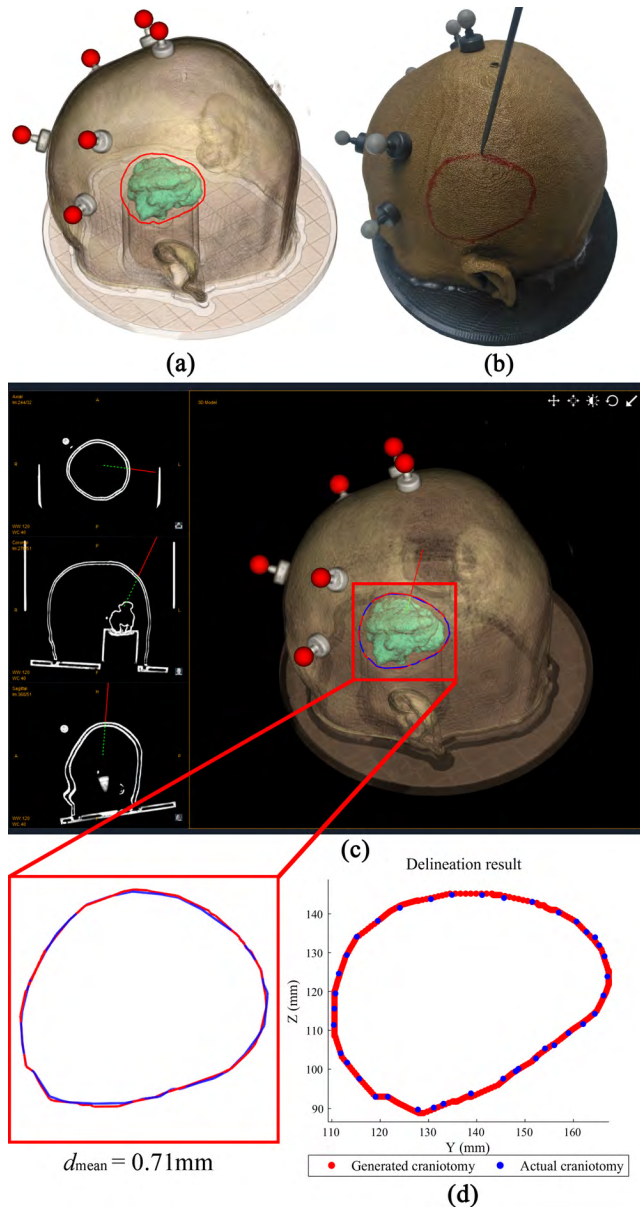
Furthermore, we located 4 craniotomies on the virtual model from 4 perspectives and draw them onto head phantom through the same way as depicted in Fig. 8. Then, the values

of d_{mean} in different perspectives were also calculated by Eq. (5). Fig. 9 shows the results of d_{mean} and the shape of two craniotomy boundaries in different cases. The mean distance d_{mean} indicates the error of craniotomy delineation and the main cause of delineation error comes from manual operation. Once the probe is far away from the generated curve by improper operation, the value of d_{mean} will be increased. In Fig. 9, the coincidence of the two craniotomies is reduced in case 1 to 4, resulting in the value of d_{mean} rises gradually. The results suggest that the mean error goes up rapidly when improper operation in drawing occurs. If the error exceeds the expected value of surgeons, the record module will remind them to redraw the curve. The value of d_{mean} can correctly reflect the concordance in two outlines of craniotomy, thus, it can be regarded as an indicator for evaluation of craniotomy delineation.

IV. DISCUSSION

The craniotomy localization in today's neurosurgical procedure requires experienced surgeons to design the skin incision according to the margin of lesion by the probe, especially in neuro-oncological surgery. Nowadays, to obtain the lesion margin, different AR-aided navigation systems were applied for overlaying the virtual lesion into the real surgical views. The silhouette of lesion can be merged into the HUD view. It is more intuitive for surgeons to observe the shape of lesion and resect the diseased tissue. Unfortunately, the 3D model would be shaken or offset in the AR-aided surgical field by marker mis-recognition, which is inconducive to surgeons designing incisions along the lesion margin. Furthermore, the lesion silhouette is just a 2D image and it is lack of spatial information to help detect whether it matches patient's scalp.

IEEE *Access*

Z. Dai *et al.*: Neurosurgical Craniotomy Localization Using Interactive 3D Lesion Mapping for Image-Guided Neurosurgery
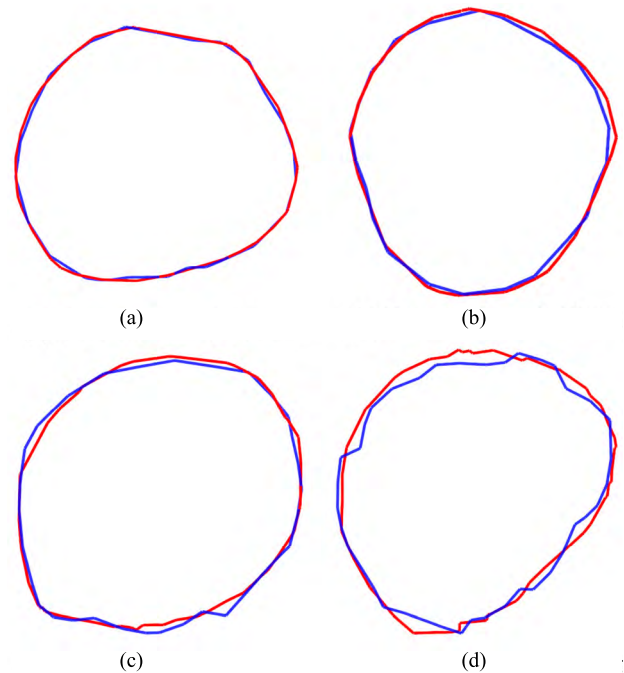

FIGURE 8. Results of craniotomy delineation: (a) craniotomy design on the virtual phantom; (b) the actual craniotomy boundary delineation on the phantom; (c) corresponding screenshot about the IGNS, the red curve is the generated craniotomy and the blue one is constructed according to the probe's movement path; (d) error analysis on YOZ plane.

FIGURE 9. The value of delineation error and the shape of two craniotomies for 4 cases.

concept, a large lesion in the depth (for example of the skull base) needs a smaller incision than a superficial lesion [1]. Thus, the purpose of our proposed method is offering a precise tool for surgeons to design an appropriate incision on actual patient's head without complex AR technology. Through above algorithms, the incision can be amended in different cases to adapt to clinical requirements. The lesion margin can be smoothed, shrinked or expanded and an appropriate craniotomy will be generated on the virtual patient's head to guide the surgeon in preoperative planning.

Additionally, compared with the "silhouette view" in AR-aided navigation system, our craniotomy has spatial information and it is composed of 3D points in world coordinate system. Applying the coordinate transformation between patient and image space, these points can be transferred to actual surgical space for providing guidance of craniotomy delineation. Nevertheless, manual incision delineation is still prone to error and intra-operator variability, resulting in large error caused by improper operation. Although the value of d_{mean} can be an indicator for evaluation of accuracy about craniotomy delineation by Eq. (5), the error cannot be controlled by algorithm and should only be controlled by surgeons. If this error exceeds the expected value, surgeons must redraw the boundary. To avoid errors caused by poor manual delineation, an ideal solution that bring in a robotic arm instead of human hands could make manual error under control. Several papers consider the use of robots to remove lesions according to a planned path [26]. Hu *et al.* [27] adopted a tissue phantom to simulate the robotic brain tumor resection based on the path planning and the results show the

Therefore, it is difficult to evaluate the performance about the preoperative incision design and intraoperative craniotomy delineation. To standardize craniotomy localization, our proposed method focuses on two issues, namely, virtual incision generation and actual craniotomy delineation and evaluation.

To generate virtual incision on the scalp model, a conformal mapping from lesion to scalp needs to be created. The reason why the mapping must be conformal is to minimize the damage to patients when the lesion would be completely removed. In general, an intracranial superficial lesion, such as meningioma, glioma and hematoma, require a lesion-consistent craniotomy. However, applying the keyhole

Z. Dai *et al.*: Neurosurgical Craniotomy Localization Using Interactive 3D Lesion Mapping for Image-Guided Neurosurgery

IEEE *Access*

RMS error between the actual path and generated is computed as 0.207mm in 3D space. It is more accurate and convenient than manual operation. However, the technology is still experimental in phantom testing and not widely available to clinical trial. Our method provides the actual coordinates of the virtual craniotomy and the coordinate transformation, which can transfer into a series of machine instructions. Then, the robot would execute these instructions to draw the craniotomy without extra manual operation. In the future, an automatic robot system will be set up to be introduced in surgical routine for precise craniotomy localization.

V. CONCLUSION

In this study, a novel interactive 3D craniotomy localization method is proposed to determine the position and size of the craniotomy on patient's head. The proposed method is capable to generate a virtual incision by lesion mapping as a reference during a preoperative planning and to provide an evaluation standard for craniotomy delineation in an ongoing image-guided surgical procedure. Since all coordinates of the craniotomy are obtained quantitatively, its size and position could be evaluated precisely. Moreover, the results of simulation demonstrate that the two outlines of craniotomies have higher concordance when eligible operations are finished. It means that our proposed method could locate a conformal craniotomy boundary and has potential to reduce the exposure of the brain.

We speculate that the standard craniotomy localization workflow has a significant effect in the future of image-guided neurosurgical operations. All data about the craniotomy could be quantified. Thus, it makes the surgical procedure will be more precise and convenient. Our future work will focus on quantifying the craniotomy amendment, researching the application of robots in image-guided neurosurgical craniotomy delineation and applying our proposed craniotomy localization method in clinical study to evaluate its performance.

REFERENCES

[1] A. T. Stadie *et al.*, "Neurosurgical craniotomy localization using a virtual reality planning system versus intraoperative image–guided navigation," *Int. J. Comput. Assist. Radiol. Surg.*, vol. 6, no. 5, pp. 565–572, Sep. 2011.

[2] P. Grunert, K. Darabi, J. Espinosa, and R. Filippi, "Computer-aided navigation in neurosurgery," *Neurosurg. Rev.*, vol. 26, no. 2, pp. 73–99, Jun. 2003.

[3] M. Kersten-Oertel, I. J. Gerard, S. Drouin, K. Petrecca, J. A. Hall, and D. L. Collins, "Towards augmented reality guided craniotomy planning in tumour resections," in *Proc. 7th Int. Conf. Med. Imag. Augmented Reality (MIAR)*. Bern, Switzerland, Aug. 2016, pp. 163–174.

[4] G. H. Barnett, R. L. Mckenzie, L. Ramos, and J. Palmer, "Nonvolumetric stereotaxy-assisted craniotomy.Results in 50 consecutive cases," *Stereotactic Funct. Neurosurg.*, vol. 61, no. 2, p. 80, Feb. 1993.

[5] I. E. Mccutcheon, "Image guided craniotomy for brain tumor," in *Textbook of Stereotactic and Functional Neurosurgery*. Berlin, Germany: Springer, 2009, pp. 699–724.

[6] J. Mcinerney and D. W. Roberts, "Frameless stereotaxy of the brain," *Mount Sinai J. Med.*, vol. 67, no. 4, pp. 300–310, Oct. 2000.

[7] W. Wagner, M. R. Gaab, H. W. S. Schroeder, and W. Tschiltschke, "Cranial neuronavigation in neurosurgery: Assessment of usefulness in relation to type and site of pathology in 284 patients," *Minimally Invasive Neurosurg.*, vol. 43, no. 3, pp. 124–131, Oct. 2000.

[8] M. Mahvash, I. Boettcher, A. K. Petridis, and T. L. Besharati, "Image guided surgery versus conventional brain tumor and craniotomy localization," *J. Neurosurg. Sci.*, vol. 61, no. 1, pp. 8–13, Jan. 2017.

[9] L. Jiang, S. Zhang, J. Yang, X. Zhuang, L. Zhang, and L. Gu, "A robust automated markerless registration framework for neurosurgery navigation," *Int. J. Med. Robot. Comput. Assist. Surg.*, vol. 11, no. 4, pp. 436–447, Dec. 2015.

[10] A. Gharabaghi *et al.*, "Image-guided craniotomy for frontal sinus preservation during meningioma surgery," *J. Surg. Oncol.*, vol. 34, no. 8, pp. 928–931, Aug. 2008.

[11] J. R. Mascitelli *et al.*, "Navigation-linked heads-up display in intracranial surgery: Early experience," *Oper. Neurosurg.*, vol. 15, no. 2, pp. 184–193, Oct. 2017.

[12] K. Asano, K. Katayama, K. Kakuta, K. Oyama, and H. Ohkuma, "Assessment of the accuracy and errors of head-up display by an optical neuronavigation system in brain tumor surgery," *Oper. Neurosurg.*, vol. 13, no. 1, pp. 23–25, Feb. 2017.

[13] T. Toyooka *et al.*, "Head-up display may facilitate safe keyhole surgery for cerebral aneurysm clipping," *J. Neurosurg.*, vol. 129, no. 4, pp. 1–7, Dec. 2017.

[14] A. Meola, F. Cutolo, M. Carbone, F. Cagnazzo, M. Ferrari, and V. Ferrari, "Augmented reality in neurosurgery: A systematic review," *Neurosurg. Rev.*, vol. 40, no. 4, pp. 1–12, May 2016.

[15] A. Xu, L. Wang, S. Feng, and Y. Qu, "Threshold-based level set method of image segmentation," in *Proc. ICINIS*, Shenyang, China, 2011, pp. 703–706.

[16] A. C. Song and D.-H. Choi, "Scale-based image enhancement using modified anisotropic diffusion filter," *Opt. Eng.*, vol. 43, no. 9, pp. 2094–2099, Sep. 2004.

[17] J. A. Sethian, "Fast marching methods," *SIAM REV.*, vol. 41, no. 2, pp. 199–235, Nov. 1999.

[18] L.-D. Chiorean, T. Szasz, M. F. Vaida, and A. Voina, "3D reconstruction and volume computing in medical imaging," *Acta Tech. Napocensis*, vol. 52, no. 3, p. 18, Sep. 2011.

[19] P. A. Nugroho, D. K. Basuki, and R. Sigit, "3D heart image reconstruction and visualization with marching cubes algorithm," in *Proc. KCIC*, Manado, Indonesia, 2016, pp. 35–41.

[20] D. Hearn, P. Baker, and W. Carithers, "Three-dimensional geometric transformations," in *Computer Graphics with OpenGL*, vol. 9, 4th ed. Englewood, NJ, USA: Prentice-Hall, 2011, pp. 301–352.

[21] J. R. Shewchuk, "Delaunay refinement algorithms for triangular mesh generation," *Comput. Geometry*, vol. 47, no. 7, pp. 741–778, May 2002.

[22] A. Perneczky and R. Reisch, "Introduction," in *Keyhole Approaches Neurosurgery*, vol. 1. Viennas, Austria: Springer, 2008, pp. 3–36.

[23] D. Ibaroudene, "Representation and display of three-dimensional medical images using a linear octree," *Comput. Med. Imag. Graph.*, vol. 19, no. 1, pp. 153–159, Dec. 1995.

[24] J. Corney, J. B. C. Davies, T. Lim, and J. M. Ritchie, "Algorithms for the physical rendering and assembly of octree models," *Comput. Aided. Des.*, vol. 38, no. 1, pp. 69–85, Jan. 2006.

[25] Q. Lin, R. Yang, K. Cai, X. Si, X. Chen, and X. Wu, "Real-time automatic registration in optical surgical navigation," *Infr. Phys. Technol.*, vol. 76, pp. 375–385, May 2016.

[26] C. Nguyen, Y. Kim, and H. Kwon, "Optimization of layout and path planning of surgical robotic system," *Int. J. Control. Autom.*, vol. 15, no. 1, pp. 375–384, Jan. 2017.

[27] D. Hu, Y. Gong, B. Hannaford, and E. J. Seibel, "Path planning for semi-automated simulated robotic neurosurgery," in *Proc. IROS*, Hamburg, Germany, 2015, pp. 2639–2645.

ZHIYU DAI received the B.S. degree in biomedical engineering from the Hefei University of Technology, Hefei, China, in 2016. He is currently pursuing the degree with the South China University of Technology, Guangzhou, China.

His main research interests include computer vision, medical image visualization, and image-guided navigation.

RONGQIAN YANG received the B.S. degree in electronic instrumentation and measurement from Nanchang Hangkong University, Nanchang, China, in 2001, the M.S. degree in communication and information systems from Jinan University, Guangzhou, China, in 2005, and the Ph.D. degree in biomedical engineering from Shanghai Jiao Tong University, Shanghai, China, in 2009.

He is currently an Associate Professor with the Department of Biomedical Engineering, South China University of Technology, Guangzhou, a Deputy Director of the Guangdong Engineering Technology Research Center for Translational Medicine of Mental Disorders, and a Visiting Associate Professor with the Department of Therapeutic Radiology, Yale University, New Haven, CT, USA. His main research areas include machine vision and biomedical instruments.

FEI HANG received the B.S. degree in materials science from Beihang University, Beijing, China, in 2006, the M.S. degree in biomaterial from the Queen Mary University of London, London, U.K., in 2007, and the Ph.D. degree from the LRC Laboratory, University of London, London, in 2010.

He is currently an Associate Professor with the Department of Biomedical Engineering and a Master Tutor with the School of Medicine, South China University of Technology, Guangzhou, China. His main research areas include biomedical 3D printing and microbiomechanics. He is a Council Member of the Royal Society for Microscopy. He is an Editor of *Frontiers in Materials*.

JIAN ZHUANG received the B.S. degree from the Department of Medicine, Southern Medical University, Guangzhou, China, in 1984, and the M.S. and Ph.D. degrees from the Department of Cardiac Surgery, Guangdong Cardiovascular Institute, Guangzhou, in 1989 and 2000, respectively. He is currently a Professor of medicine with the Department of Cardiac Surgery, Guangdong General Hospital and School of Medicine, South China University of Technology, Guangzhou.

His main research interests include surgery navigation in heart disease and 3D printing technology in medicine.

QINYONG LIN received the B.S. and Ph.D. degrees in biomedical engineering from the South China University of Technology, Guangzhou, China, in 2010 and 2016, respectively, where he is currently a Postdoctoral Researcher.

His main research interests include computer vision, surgical robots, and image-guided navigation.

ZHIGANG WANG received the B.S. degree in biomedical engineering from Nanchang Hangkong University, Nanchang, China, in 2009, and the M.S. degree in biomedical engineering from the South China University of Technology, Guangzhou, China, in 2012. He is currently with Guangzhou Aimooe Technology Co., Ltd.

His main research interests include surgical navigation systems and surgery robots.

YONGHUA LAO received the B.S. degree in generating machine engineering, the M.S. and Ph.D. degrees in biomedical engineering from the South China University of Technology, Guangzhou, Guangdong, China, in 2001, 2003, and 2010, respectively.

He is currently a Lecturer with the Department of Biomedical Engineering, South China University of Technology. His main research areas include biomedical instruments, biomodels, and biomechanics.

● ● ●